Atmósfera 38, 369-380 (2024)
https://doi.org/10.20937/ATM.53270

Carbonaceous particles and $PM_{2.5}$ optical properties in Mexico City during the ACU15 campaign

Naxieli SANTIAGO-DE LA ROSA[1], Cristina PRIETO[2], Rubén PAVIA[2], Óscar PERALTA[1]*, Harry ÁLVAREZ-OSPINA[3], Isabel SAAVEDRA[1], Telma CASTRO[1], Rocío GARCÍA[1], María de la Luz ESPINOSA[1], Abraham ORTÍNEZ-ÁLVAREZ[4], Gerardo RUIZ-SUÁREZ[1] and Amparo MARTÍNEZ-ARROYO[1]

[1] *Instituto de Ciencias de la Atmósfera y Cambio Climático, Universidad Nacional Autónoma de México, Circuito Exterior s/n, Ciudad Universitaria, 04510 Ciudad de México, México.*
[2] *Posgrado en Ciencias de la Tierra, Universidad Nacional Autónoma de México, Circuito Exterior s/n, Ciudad Universitaria, 04510 Ciudad de México, México.*
[3] *Facultad de Ciencias, Universidad Nacional Autónoma de México, Circuito Interior s/n, Ciudad Universitaria, 04510 Ciudad de México, México.*
[4] *Instituto Nacional de Ecología y Cambio Climático, Carretera Picacho-Ajusco 4219, Jardines en la Montaña, 14210 Ciudad de México, México.*
*Corresponding author; email: oscar@atmosfera.unam.mx

Received: March 5, 2023; Accepted: September 29, 2023

RESUMEN

Medimos las propiedades ópticas de aerosoles con dos espectrómetros fotoacústicos que operaban a longitudes de onda de 532 y 870 nm y tomamos muestras de $PM_{2.5}$ para analizar el contenido de carbono orgánico (OC, por su sigla en inglés) y carbono elemental (EC). El sitio de medición estaba en la esquina suroeste de la Ciudad de México. Ordenamos los datos por cocientes OC/EC y calculamos cuatro eficiencias de absorción de masa (MAE) para cada longitud de onda. Los diferentes MAE variaron de 2.27 a 19.75 $m^2\ g^{-1}$ a 532 nm y 2.03-15.26 $m^2\ g^{-1}$ a 870 nm, con coeficientes de determinación superiores a 0.88, lo que demuestra que la cantidad de OC modifica las propiedades de absorción de las partículas, en ocasiones subestimando o sobreestimando la concentración de carbono negro. Se puede elegir un MAE con base en la concentración mediana diaria de O_3 si no hay información sobre la composición de EC y OC de los aerosoles atmosféricos.

ABSTRACT

We measured the optical properties of aerosols with two photoacoustic spectrometers operating at 532 and 870 nm wavelengths and sampled $PM_{2.5}$ to analyze the organic carbon (OC) and elemental carbon (EC) content. The measuring site was in the southwest corner of Mexico City. We sorted the data by OC/EC ratios and calculated four mass absorption efficiencies (MAEs) for each wavelength with linear regressions. The MAEs ranged from 2.27 to 19.75 and 2.03 to 15.26 $m^2\ g^{-1}$ at 532 and 870 nm, respectively, with determination coefficients above 0.88, showing that the amount of OC modifies the absorption properties of particles, sometimes underestimating or overestimating the black carbon concentration. It is possible to choose the MAE based on the daily median O_3 concentration when there is no information about the EC and OC composition.

Keywords: mass absorption efficiency, elemental carbon, carbonaceous aerosols, Mexico City, $PM_{2.5}$.

1. Introduction

The emission of particles derived from anthropogenic activities into the atmosphere affects the hydrological cycle, air quality, and global radiative balance (Ramanathan and Carmichael, 2008). Since atmospheric particles absorb and scatter light, they lead to changes in energy and temperature in the environment (Horvath, 1993); hence, the terrestrial radiation budget and global warming are intimately connected with atmospheric aerosols. Furthermore, in polluted urban atmospheres, particulate matter with an aerodynamic diameter of 2.5 μm or less ($PM_{2.5}$) contains black carbon (BC), a critical short-life climate forcer. That is why some countries have included BC within their mitigation agendas.

The incomplete combustion of coal, trash, biomass, and fossil fuels produces gases and particles containing BC and other light-absorbing substances (Paredes-Miranda et al., 2009; Aiken et al., 2010). BC absorbs light efficiently at all visible wavelengths, but other carbonaceous substances (i.e., brown carbon, BrC) prefer UV and short wavelengths (Li et al., 2020). Although particles with BC are slowly reacting in the atmosphere, they interact with many other species leading to changes in optical properties (Peng et al., 2016). For instance, some authors have found fractal soot particles with non-absorbing material that modifies the particle's physical, hygroscopic, and optical properties (Weingartner et al., 2003).

BC and elemental carbon (EC) are usually interchangeable terms, despite different analytical methods supporting the definitions of each species. Instruments measure BC based on the absorption coefficient of particles, and EC is measured with thermochemical analyses (Pöschl, 2005). The link between light absorption (b_{abs}) and BC/EC abundance is the mass absorption cross-section or mass absorption efficiency (MAE) (Cheng et al., 2011; Tao et al., 2018; Cappa et al., 2019); however, it depends on particle size, aging, mixing state, coating distribution of species, and other particle factors (Knox et al., 2009), so it is hardly a constant value due to the diversity and complexity of atmospheric particles in nature. We have defined the MAE as the optical interaction of a chemical compound in the particle (in this case, elemental carbon) with solar radiation.

Some air quality networks determine BC concentrations with monitors that measure the optical properties of the particle because it is faster and cheaper than chemical techniques and there is sometimes a bias, since instruments assume that BC is the only absorber and the particle has a constant MAE. Aerosols from Mexico City contain around 50% by mass of carbonaceous compounds (Torres-Jardón et al., 2009; Peralta et al., 2019) and this quantity may alter the optical properties of the particle.

The atmosphere of Mexico City is under a volatile organic compound regime. It is a highly reactive system due to ozone and other oxidants in the air that probably accelerate aging processes and modify the optical properties of the particles (García-Reynoso et al., 2009; Peralta et al., 2021). We measured the light absorption (b_{abs}) and scattering (b_{sca}) coefficients of $PM_{2.5}$ at two wavelengths, sampled $PM_{2.5}$, quantified EC and organic carbon (OC) content, and described aerosol MAE changes as a function of the CO/CE ratio. The different values of MAE will reduce the uncertainty of BC measurements in cities of developing countries.

2. Method and instruments

The measurement campaign took place at the Instituto de Ciencias de la Atmósfera y Cambio Climático (Institute for Atmospheric Sciences and Climatic Change, ICAyCC) building on the Universidad Nacional Autónoma de México (National Autonomous University of Mexico, UNAM) campus, from January 19 to March 20, 2015, as a part of the Atmospheric Aerosols Campaign at University Campus (ACU15) within the Air Quality Project Study in Central Mexico (ECAIM) (Salcedo et al., 2018).

2.1 Meteorology

The Red Universitaria de Observatorios Atmosféricos (University Network of Atmospheric Observatories, RUOA) and the Programa de Estaciones Metereológicas del Bachillerato Universitario (University Program of High School Meteorological Stations, PEMBU) provided the meteorological data (wind speed and direction, temperature, solar radiation, pressure, and relative humidity) for the campaign. PEMBU has Vantage Pro 2 weather monitoring stations (Davis Instruments). Data can be consulted at https://www.ruoa.unam.mx/pembu/index.php?page=historical_facts

2.2 Particle optical properties

The instruments were located on the roof of the ICAyCC building, and the sampling probe was 5 m above the roof and 10 m above the ground to avoid resuspended soil particles. We used a photoacoustic spectrometer (PAS) and a photoacoustic extinctiometer (PAX) to measure the optical properties of $PM_{2.5}$. Both instruments operated continuously from January 21 to February 6 and from February 17 to March 21, 2015. We connected both instruments to a TSI aerosol splitter and then to a 2.5 µm cyclone (URG). PAS and PAX sampled aerosols with a flow rate of 1.0 l min^{-1}.

PAS and PAX have the same operation principle, where the quantity of absorption measured is proportional to the sound pressure produced in an acoustic resonator caused by the absorption of light. The acoustic resonator operates in plane wave mode with a resonant frequency of 500 Hz and a photoacoustic coefficient of 12.8 Pa (W m^{-1}). The coherent acoustic noise is suppressed with filters at the pressure nodes of the resonator. The laser wavelengths selected for the photoacoustic spectrometers avoid absorption of gaseous atmospheric light, with a gaseous absorption coefficient of 0.1 Mm^{-1} (Liñán-Abanto et al., 2021). The instruments have also a wide-angle integrating reciprocal nephelometer to measure the scattering coefficient of light.

The lower detection limit for light absorption is 0.4 Mm^{-1}, which corresponds to a mass density of elemental carbon of 40 ng m^{-3}, assuming a light absorption efficiency of 10 m^2 g^{-1}. Also, the absorption and scattering coefficients of atmospheric gases like O_2, NO_2, O_3, and H_2O are two orders of magnitude lower compared to those of aerosols (Horvath, 1993).

The University of Nevada built the PAS, which has a laser operating at 532 nm (Arnott et al., 1999). The PAX is a commercial model (Droplet Measurement Technologies, USA) with a laser operating at 870 nm. Both spectrometers recorded the particle's optical properties (absorption, scattering, and extinction coefficients) every minute. PAX also quantified BC using a default mass absorption efficiency (MAE) of 4.74 m^2 g^{-1} (Prieto et al., 2023). The intercomparison of PAS and PAX data had a good determination coefficient (R^2 = 0.97).

2.3 $PM_{2.5}$ sampling

Before sampling, 47 mm quartz filters (Tissue quartz 2500QAT-UO, 47 mm, PALL) were preheated at 600 ºC for 6 h to eliminate the organic material that could be present. Then, we conditioned the substrates for 24 h at constant relative humidity (less than 30%) and 25 ºC, weighed them on an analytical balance (Sartorius CPA225D-OCE), and boxed them individually in plastic Petri dishes. The plastic dishes were wrapped with parafilm tape and opened until the sampling time. Filters after sampling were stored at 4 ºC, stabilized for 24 h at the same conditions as before and weighed.

We calibrated the Minivol sampler (Airmetrics) flow rate with a Gillibrator at a constant 5.0 L min^{-1}. The impactor collected $PM_{2.5}$ on filters every 24 h. The Red Automática de Monitoreo Atmosférico (Automatic Atmospheric Monitoring Network, RAMA) of Mexico City provided continuous $PM_{2.5}$ concentrations, with a Thermo Andresen model FH62C14 continuous particulate monitor based on beta attenuation.

2.4 Carbon analysis

The carbon analyzer CM5014 (UIC) measures OC and total carbon (TC) content. The instrument quantifies CO_2 produced from the complete combustion of carbonaceous material in a coulombimetric cell and converts it into carbon content. We calibrated the instrument with NIST SRM 1649a Urban Dust (Álvarez-Ospina et al., 2016). OC evolved at 450 ºC and TC at 700 ºC. The difference between TC and OC corresponds to elemental carbon (EC), following Eq. (1):

$$EC = TC - OC \tag{1}$$

2.5 Optical properties and statistical analysis

We measured the particle's absorption and scattering coefficients every minute and averaged the values for 24 h to match the optical property databases with those of OC and EC analyses. With the daily averages, we calculated the MAE_{532} (532 nm) and MAE_{870} (870 nm) according to Eq. (2), which represents the ratio of particle absorption coefficient and the concentration of light-absorbing chemical species, basically EC. We also calculated the single scattering albedo (SSA) with Eq. (3):

$$MAE = \frac{b_{abs}}{EC} \tag{2}$$

$$SSA = \frac{b_{sca}}{b_{ext}} \quad (3)$$

We applied a linear regression of b_{abs} as a function of EC, where the slope corresponds to the MAE ($m^2\ g^{-1}$). To contrast the hypothesis of normality, we used the Kolmogorov-Smirnov statistical test ($\alpha = 0.05$). The data had a non-parametric distribution; hence, we applied the Mann-Whitney statistical test to compare b_{abs} and EC.

3. Results

3.1 Meteorology

January, February, and March are part of the cold-dry season in Mexico City, and cold air masses often blow from the S-SW to the city. Southerly winds are associated with air masses containing low temperatures and high relative humidity. These air masses are not polluted, unlike those coming from the north, where the industrial area of Mexico City is located.

From January to mid-March the mean wind speed was 1.8 m s^{-1}. Wind speed was slow, so we believe local activities produced most of the airborne particles. By March 15, the average wind speed increased to 3.0 m s^{-1} (Fig. 1). In January and February, the W-NW wind direction prevailed and in the week of March 8 to 15, the wind changed its direction and blew from the south (Fig. 1). From January 19 to February 15, the average temperature was 13.9 ± 1.5 ºC and from March 8 it increased to 17.8 ± 1.6 ºC (Fig. 1). From January 19 to March 8 relative humidity was 50% and after March 8 it increased to 60% with southerly winds. Figure 1 shows the basic meteorological parameters (wind speed and direction, temperature, and relative humidity) recorded in the measurement campaign.

3.2 Particle optical properties

At 532 nm, the average b_{abs} was 13.68 ± 6.89 Mm^{-1}, and at 870 nm it was 10.40 ± 5.33 Mm^{-1}. From January 18 to 31, it decreased as the wind intensity increased. In February, b_{abs} varied from one week to another, ranging from 7.25 to 21.92 Mm^{-1} (532 nm) and from 5.10 to 17.44 Mm^{-1} (870 nm). From March 8 to 15, it decreased as the wind speed went up (Fig. 2).

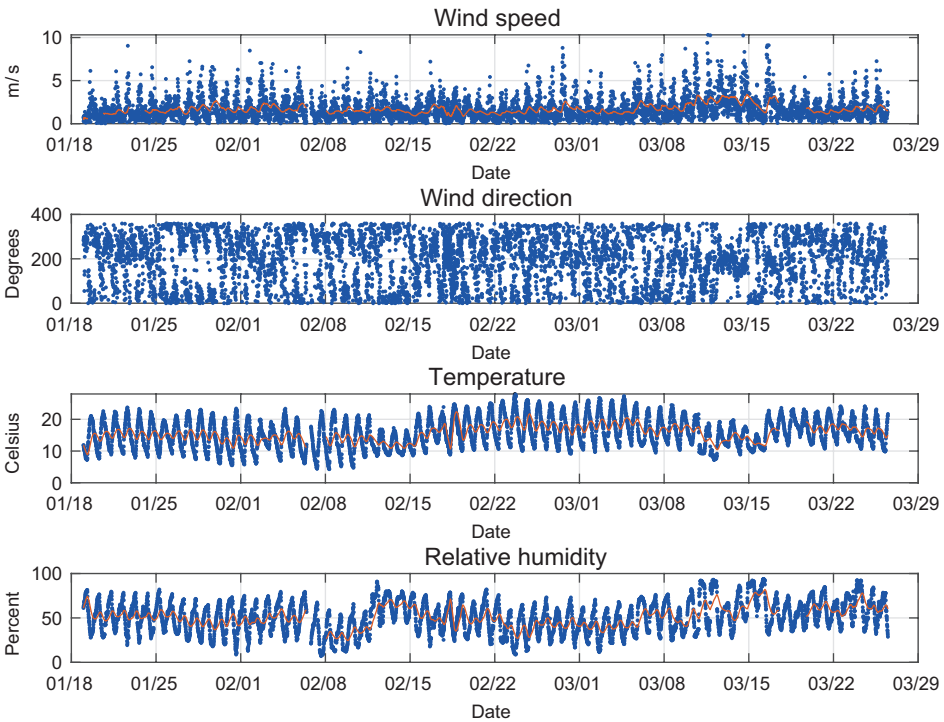

Fig. 1. Time series of meteorological parameters: wind speed, temperature, wind direction, and relative humidity. Red thin lines are the 24-h moving averages.

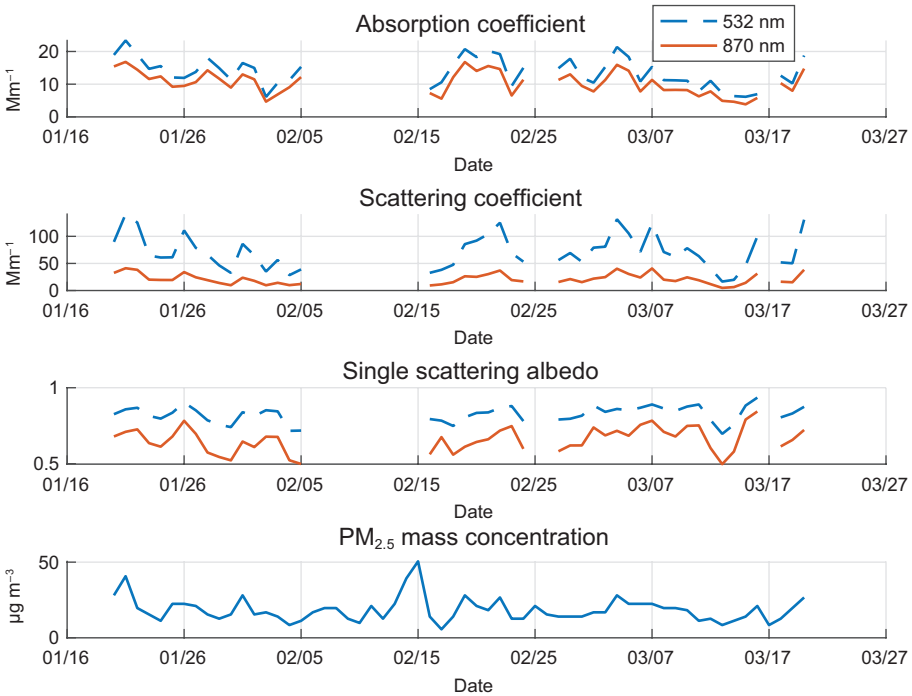

Fig. 2. Particle's optical properties: absorption coefficient, scattering coefficient, single scattering albedo, and $PM_{2.5}$. Dotted blue lines correspond to the 532 nm wavelength and orange lines to 870 nm.

The average b_{sca} was 71.00 ± 40.56 Mm^{-1} at 532 nm and 21.37 ± 12.31 Mm^{-1} at 870 nm. Between January 21 and February 6, the scattering decreased to half of its average value, with the wind blowing from N-NW, probably transporting pollutants from the industrial part of the city. From March 8-15, b_{sca} decreased associated with a cold front entering Mexico City (Fig. 2).

At both wavelengths, the SSA reached its minimum value at 07:00, when light absorption was at its maximum produced by the presence of dark particles. The SSA_{532} maximum was 0.89, and the SSA_{870} maximum was 0.77, around 13:00 LT, when the absorption coefficient dropped to its minimum value (Prieto et al., 2023). The average SSA_{532} was 0.83 ± 0with.35 Mm^{-1} and the average SSA_{870} was 0.66 ± 0.28 Mm^{-1}. The difference in values is probably due to more chemical species in the particle being sensitive to lower wavelengths.

Particles are covered with different materials, oxidated species, water, and other coating substances changing the particle optical properties and promoting the formation of secondary aerosols. Furthermore, SSA_{532} values were close to 1.0 (Fig. 2), probably linked to secondary aerosols and other materials that scatter light (Eck et al., 1999; Cheng et al., 2011; Schumann, 2012; Tao et al., 2019).

3.3 Carbon content

The average mass concentration of $PM_{2.5}$ was 18.45 ± 8.00 μg m^{-3}, while the average concentration of OC was 7.96 ± 3.61 μg m^{-3}, and for EC it was 2.44 ± 1.77 μg m^{-3}. So, EC corresponded to 12% and OC to 39% of the total $PM_{2.5}$ mass, which means that the carbonaceous material is 51% of the particle mass. Vehicles and commercial activities were probably the main sources of emission of carbonaceous material near the sampling site. The carbon composition had significant variations, perhaps due to the contribution of various sources and secondary atmospheric processes. The correlation coefficient between OC and EC was 0.10. The average OC/EC ratio ranged from 1.08 to 22.89, with a mean of 5.58 ± 1.08 (Turpin et al., 1990; Chow et al., 2011).

The was 1.08, and primary organic carbon (POC) was calculated following Eq. (4). We used Eq. (5) to calculate secondary organic carbon (SOC) (Castro et al., 1999). SOC average concentration was 5.32 ± 2.96 µg m^{-3}, meaning that the secondary species contribution was more significant than POC. SOC is linked to temperature, but the statistical analysis concludes that there is no significant difference between SOC concentrations and monthly temperature (Zhang et al., 2013). In January, February, and March, the average temperature was 14.54, 14.94, and 15.88 ºC, respectively.

$$\mathrm{POC} = \left(\frac{OC}{EC}\right)_{min} {}^{*}EC \tag{4}$$

$$SOC = OC - POC \tag{5}$$

Figure 3 shows the daily variations of organic carbon (POC and SOC) and EC. Variations in POC and SOC concentrations are likely due to changes in emission sources, transport of airborne material, or secondary processes in the atmosphere.

3.4 Mass absorption efficiency (MAE)

MAE efficiency corresponds to the ratio of daily average absorption coefficient and EC concentration, following Eq. (2). The range of MAE_{532} was 0.11-2.44 m^2 g^{-1} with an average value of 0.59 ± 0.57 m^2 g^{-1}. The range of MAE_{870} was 1.39-25.60 m^2 g^{-1}, with an average value of 6.78 ± 5.85 m^2 g^{-1}. The PAX uses a default MAE of 4.74 m^2 g^{-1} that falls into the average MAE_{870}.

The EC concentration and the daily average b_{abs} changed from one day to another, probably caused by changes in the emission rates of local sources, transport, or atmospheric aging processes. Hence, MAE at both wavelengths had considerable variations, and the correlation coefficients of EC versus b_{abs} were 0.41 (at 532 nm) and 0.39 (at 870 nm).

We sorted the data by OC/EC ratios in four groups assuming an external mixing of the particle. We assumed EC was the only absorbing material in the particle at both wavelengths and different concentrations of scattering material modified the absorbing properties of EC, like a shadowing effect (Weingartner et al., 2003). Then we calculated the

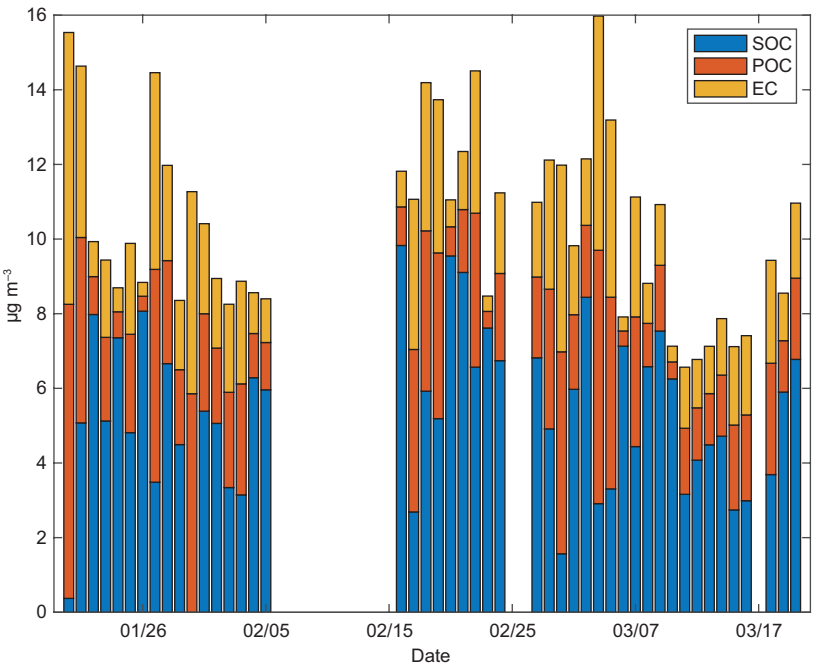

Fig. 3. Carbon content in $PM_{2.5}$ samples. Primary organic carbon (POC) and secondary organic carbon (SOC) were calculated following Eqs. (7) and (8). (EC: elemental carbon.)

Table I. OC/EC ratio groups and linear regression equations.

Group	OC/EC ratio range	n	y = mx	MAE (m^2 g^{-1})	R^2	SOC/POC range
Wavelength: 532 nm						
1	OC/EC < 2.0	6	y = 19.75x	19.75	0.88	0.00 – 0.64
2	2.0 < OC/EC < 3.1	14	y = 7.75x	7.75	0.94	1.02 – 1.83
3	3.1 < OC/EC < 8. 0	19	y = 4.46x	4.46	0.97	2.06 – 5.67
4	OC/EC > 8.0	8	y = 2.67x	2.67	0.97	7.88 – 20.16
Wavelength: 870 nm						
5	OC/EC < 2.0	6	y = 15.26x	15.26	0.89	0.00 – 0.64
6	2.0 < OC/EC < 3.1	14	y = 5.95x	5.95	0.94	1.02 – 1.83
7	3.1 < OC/EC < 8.0	19	y = 3.37x	3.37	0.97	2.06 – 5.67
8	OC/EC > 8.0	8	y = 2.03x	2.03	0.97	7.88 – 20.16

OC: organic carbon; EC: elemental carbon; MAE: mass absorption efficiency; SOC: secondary organic carbon; POC: primary organic carbon.

linear regression for each group of data. Groups 1 and 5 corresponded to OC/EC ratios < 2.0, where OC and EC concentrations were similar. Groups 2 and 6 were for OC/EC ratios between 2.0 and 3.1. Groups 3 and 7 comprised OC/EC ratios between 3.1 and 8.0. Groups 4 and 8 were for particles with a notable predominance of organic compounds, with OC/EC ratios greater than 8.0. Table I shows the OC/EC ratio ranges, the population, the linear regression equation, and the determination coefficient for each group. Figure 4 shows the data and linear adjustment for each group. All regressions intersect the b_{abs} axis

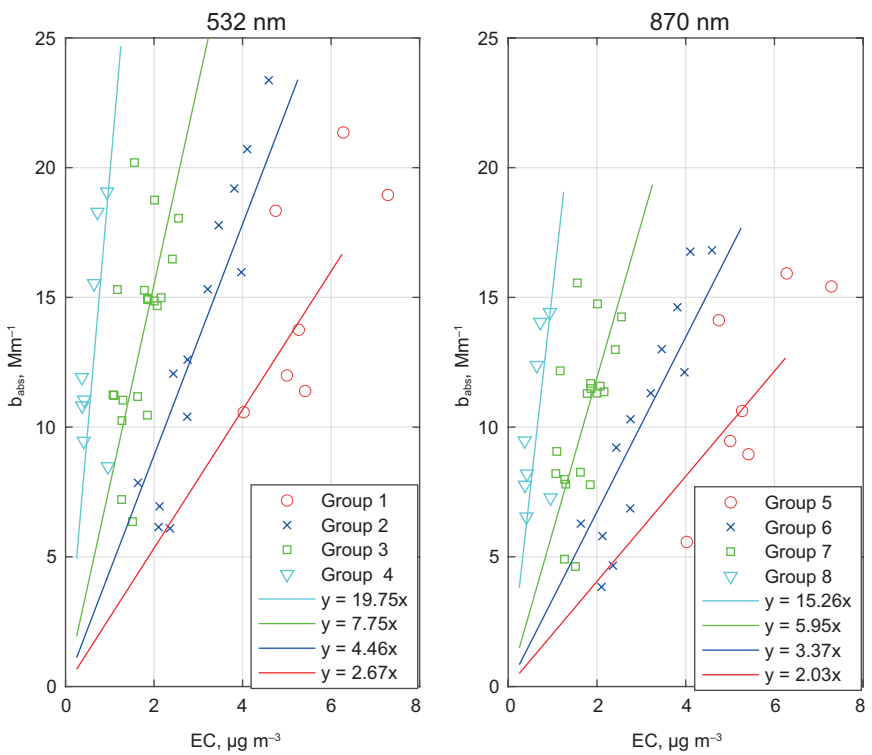

Fig. 4. Scatter plots of elemental carbon (EC) and light absorption (b_{abs}) grouped by different OC/EC ratios, where MAE corresponds to the slope of the regression lines, at 532 nm and at 870 nm. (OC: organic carbon.)

at EC = 0 because we assumed EC was the unique contribution to light-absorbing in the particle and OC modified the light-absorbing properties of EC but did not absorb light directly.

The carbonaceous material, with a high contribution of OC and other species, changed the optical properties of aerosols, and the amount of primary and secondary organic compounds modified the aerosols' absorbing light capacity. When the amount of OC was like EC in the particle (OC/EC ratio < 2.0), we had a MAE_{532} of 19.75 $m^2 g^{-1}$, and MAE_{870} was 15.26 $m^2 g^{-1}$. As the amount of OC increased MAE diminished, and if the OC concentration was eight times the EC mass (OC/EC ratio > 8.0), then the MAE_{532} was equal to 2.67 $m^2 g^{-1}$, and the MAE_{870} was 2.03 $m^2 g^{-1}$.

4. Discussion

Activities at the UNAM campus, as well as nearby commercial areas and vehicles, impact the measuring site by emitting particles. The SSA suggests the presence of particulate matter with a significant coating of scattering substances since values are 0.82 at 532 and 0.66 at 880 nm at noon. SSA is linked to the radiative energy budget, and those values show the variety of absorbing and scattering material in urban aerosols.

It is also possible to find aerosols with a large and thick coat of scattering material like water and organic or inorganic compounds. Authors mention that the aging processes of aerosols modify the BC light absorption capacity, as observed in Mexico City (Salcedo et al., 2018) and in China (Wang et al., 2018, 2020). We found a large amount of OC in particles, probably resulting from natural and human atmospheric sources.

Linear regressions of the different groups show high determination coefficients ($R^2 > 0.85$), meaning that organic compounds are important in the particle's interaction with light. Table II shows MAE from other studies for comparison with the results shown in Table I. MAE values shown in Table II do not have an increasing sequence as the OC/EC ratio decreases. The samples were collected in different environments, and the particle optical properties were measured at different wavelengths.

The OC average concentration was three times higher than EC, and there were days when the OC fraction reached eight times the EC. OC is primary and secondary, and the OC/EC ratios change MAE_{532} and MAE_{870}. The absorbing material of the particle probably has both BC and BrC; the first species is associated with vehicular activities and is sensitive to detection at 870 nm. The 532 nm wavelength is

Table II. Some MAE reported in other studies and the OC/EC ratios.

OC/EC reported by other authors	MAE reported by other authors	Wavelength	Source	Reference
8.17	8.11 (EC)	880 nm	Biomass burning	(Tao et al., 2020)
	0.24 (OC)			
8.50	11.3 (EC)	660 nm	Urban	(Ram and Sarin, 2009)
2.94	1.00 (WSOC)	700 nm	Urban	(Li et al., 2019)
17.62	6.10 (EC)	632 nm	Biomass Burning	(Hu et al., 2017)
1.19	8.10 (EC)		Vehicle emissions	
2.8	0.3 (WSOC)	365 nm	Urban	(Srinivas and Sarin, 2013)
1.5	0.3 (WSOC)			
0.7	0.2 (WSOC)			

OC: organic carbon; EC: elemental carbon; MAE: mass absorption efficiency; SOC: secondary organic carbon; POC: primary organic carbon; WSOC: water-soluble organic carbon. Abbreviations in parentheses indicate that compounds were used to calculate MAE.

commonly used to detect BrC from biomass sources (i.e., natural emissions and biomass burning, among others). However, in our case, we adjusted both wavelengths to detect only EC, which is a chemical species that we can analyze with thermochemical techniques.

Since the OC/EC ratio modifies the particle's optical properties, it affects BC measurements underestimating or overestimating its concentration during the day. Based on a constant $MAE_{870} = 4.74\ m^2\ g^{-1}$ (like PAX), the underestimation reaches 75% if the OC/EC ratio is below 2.0, and the overestimation is close to 100% if the OC/EC ratio is above 8.0. The determination of BC based on the particle optical properties and OC/EC ratios is probably influenced by emissions from different sources of combustion (gasoline, diesel, biomass, among others), meteorological changes (i.e., relative humidity, temperature), and other atmospheric reactants.

If the emission rates of pollutants and the photo-oxidation processes in the atmosphere change on time modifying the particle optical properties, it is not easy to estimate a general MAE without chemical analyses of both OC and EC. Some authors find that O_3 is a proxy of SOC presence (Turpin and Huntzicker, 1995). Figure 5 (upper panel) shows BC readings by PAX, BC corrected by MAE_{870}, and EC, and the same figure (lower panel) shows the OC/EC ratio and the daily median of O_3. There is a tendency to have high OC/EC ratios with O_3 concentrations above 30 ppb, but this does not always happen.

Groups 1 and 5 have an OC/EC ratio below 2.0, and their SOC/POC ratio is lower than 1.0, so they probably correspond to fresh particles emitted from a specific source.

5. Conclusions

Based on the SOC/POC ratio and the the measuring site is a receptor point with aging aerosols prevailing over newly emitted particles, where OC is the predominant species, capable of modifying the light absorption properties of absorbing species (assuming

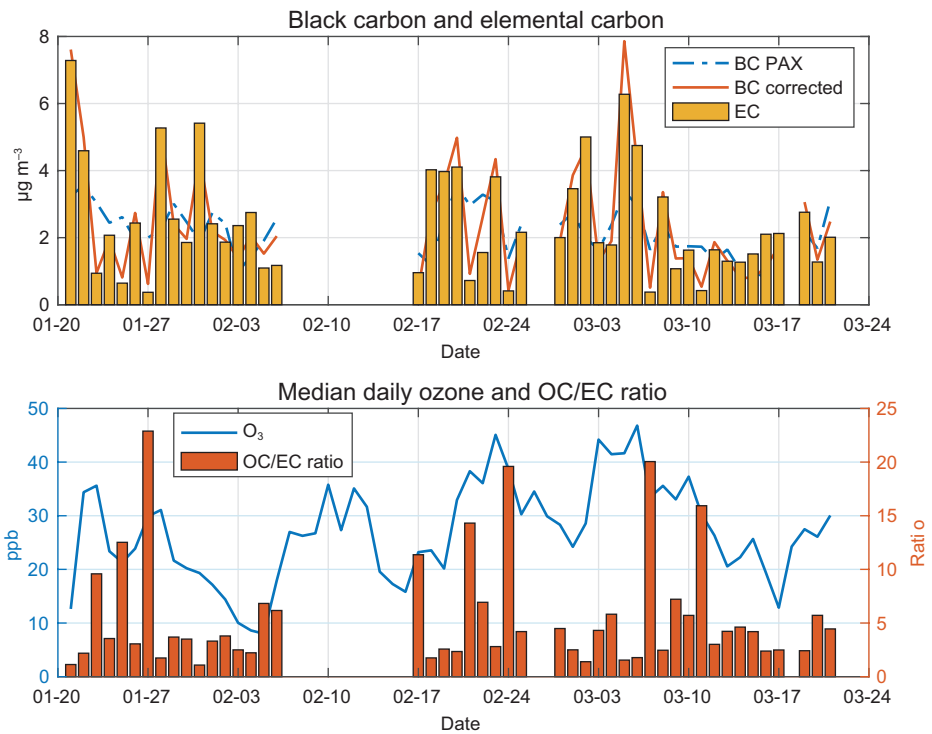

Fig. 5. Upper panel: EC concentrations (bars), BC concentrations estimated with PAX ($MAE = 4.74\ m^2\ g^{-1}$), and BC corrected with the new MAE for different OC/EC ratios. Lower panel: median daily O_3 concentration and OC/EC ratio. (EC: elemental carbon; BC: black carbon; PAX: photoacoustic extinctiometer; MAE: mass absorption efficiency).

EC is the only absorbing species). The particle undergoes daily transformations, modifying its optical properties. The MAEs obtained by other authors show a variety of values since they depend on the measuring wavelength, the type of carbonaceous compounds, and the predominant particle source. However, other reactive species, like O_3, can operate as a proxy for the presence of SOC.

Acknowledgments

Authors want to thank the ECAIM project for the support and facilities granted during the campaign and the ICAyCC for all the help and materials offered for this project.

References

Aiken AC, De Foy B, Wiedinmyer C, Decarlo PF, Ulbrich IM, Wehrli MN, Szidat S, Prevot ASH, Noda J, Wacker L, Volkamer R, Fortner E, Wang J, Laskin A, Shutthanandan V, Zheng J, Zhang R, Paredes-Miranda G, Arnott WP, Molina LT, Sosa G, Querol X, Jiménez JL. 2010. Mexico City aerosol analysis during MILAGRO using high resolution aerosol mass spectrometry at the urban supersite (T0) – Part 2: Analysis of the biomass burning contribution and the non-fossil carbon fraction. Atmospheric Chemistry Physics 10: 5315-5341. https://doi.org/10.5194/acp-10-5315-2010

Álvarez-Ospina H, Peralta O, Castro T, Saavedra MI, 2016. Optimum quantification temperature for total, organic, and elemental carbon using thermal-coulombimetric analysis. Atmospheric Environment 145: 74-80. https://doi.org/10.1016/j.atmosenv.2016.08.080

Arnott WP, Moosmüller H, Rogers CF, Jin T, Bruch R. 1999. Photoacoustic spectrometer for measuring light absorption by aerosol: Instrument description. Atmospheric Environment 33: 2845-2852. https://doi.org/10.1016/S1352-2310(98)00361-6

Cappa CD, Zhang X, Russell LM, Collier S, Lee AKY, Chen C-L, Betha R, Chen S, Liu J, Price DJ, Sanchez KJ, McMeeking GR, Williams LR, Onasch TB, Worsnop DR, Abbatt J, Zhang Q. 2019. Light absorption by ambient black and brown carbon and its dependence on black carbon coating state for two California, USA, cities in winter and summer. Journal of Geophysical Research: Atmospheres 124: 1550-1577. https://doi.org/10.1029/2018JD029501

Castro LM, Pio CA, Harrison RM, Smith DJT. 1999. Carbonaceous aerosol in urban and rural European atmospheres: Estimation of secondary organic carbon concentrations. Atmospheric Environment 33: 2771-2781. https://doi.org/10.1016/S1352-2310(98)00331-8

Cheng Y, He K-B, Zheng M, Duan F-K, Du Z-Y, Ma Y-L, Tan J-H, Yang F-M, Liu J-M, Zhang X-L, Weber RJ, Bergin MH, Russell AG. 2011. Mass absorption efficiency of elemental carbon and water-soluble organic carbon in Beijing, China. Atmospheric Chemistry Physics 11: 11497-11510. https://doi.org/10.5194/acp-11-11497-2011

Chow JC, Watson JG, Lowenthal DH, Antony Chen LW, Motallebi N. 2011. $PM_{2.5}$ source profiles for black and organic carbon emission inventories. Atmospheric Environment 45: 5407-5414. https://doi.org/10.1016/j.atmosenv.2011.07.011

Eck TF, Holben BN, Reid JS, Dubovik O, Smirnov A, O'Neill NT, Slutsker I, Kinne S. 1999. Wavelength dependence of the optical depth of biomass burning, urban, and desert dust aerosols. Journal of Geophysical Research: Atmospheres 104: 31333-31349. https://doi.org/10.1029/1999JD900923

García-Reynoso A, Jazcilevich A, Ruiz-Suárez LG, Torres-Jardón R, Suárez Lastra M, Reséndiz Juárez NA. 2009. Ozone weekend effect analysis in Mexico City. Atmósfera 22: 281-297.

Horvath H. 1993. Atmospheric light absorption – A review. Atmospheric Environment. Part A. General Topics 27: 293-317. https://doi.org/10.1016/0960-1686(93)90104-7

Hu W, Hu M, Hu WW, Zheng J, Chen C, Wu Y, Guo S. 2017. Seasonal variations in high time-resolved chemical compositions, sources, and evolution of atmospheric submicron aerosols in the megacity Beijing. Atmospheric Chemistry and Physics 17: 9979-10000. https://doi.org/10.5194/acp-17-9979-2017

Knox A, Evans GJ, Brook JR, Yao X, Jeong C-H, Godri KJ, Sabaliauskas K, Slowik JG. 2009. Mass absorption cross-section of ambient black carbon aerosol in relation to chemical age. Aerosol Science and Technology 43: 522-532. https://doi.org/10.1080/02786820902777207

Li X, Jiang L, Bai Y, Yang Y, Liu S, Chen X, Xu J, Liu Y, Wang Y, Guo X, Wang Y, Wang G. 2019. Wintertime aerosol chemistry in Beijing during haze period: Significant contribution from secondary formation and biomass burning emission. Atmospheric Research 218: 25-33. https://doi.org/10.1016/j.atmosres.2018.10.010

Li X, Wang Y, Hu M, Tan T, Li M, Wu Z, Chen S, Tang X. 2020. Characterizing chemical composition and light absorption of nitroaromatic compounds in the winter of Beijing. Atmospheric Environment 237: 117712. https://doi.org/10.1016/j.atmosenv.2020.117712

Liñán-Abanto RN, Salcedo D, Arnott P, Paredes-Miranda G, Grutter M, Peralta O, Carabali G, Serrano-Silva N, Ruiz-Suárez LG, Castro T. 2021. Temporal variations of black carbon, carbon monoxide, and carbon dioxide in Mexico City: Mutual correlations and evaluation of emissions inventories. Urban Climate 37: 100855. https://doi.org/10.1016/j.uclim.2021.100855

Paredes-Miranda G, Arnott WP, Jiménez JL, Aiken AC, Gaffney JS, Marley NA. 2009. Primary and secondary contributions to aerosol light scattering and absorption in Mexico City during the MILAGRO 2006 campaign. Atmospheric Chemistry and Physics 9: 3721-3730. https://doi.org/10.5194/acp-9-3721-2009

Peng J, Hu M, Guo S, Du Z, Zheng J, Shang D, Levy-Zamora M, Zeng L Shao M, Wu YS, Zheng J, Wang Y, Glen CR, Collins DR, Molina MJ, Zhang R. 2016. Markedly enhanced absorption and direct radiative forcing of black carbon under polluted urban environments. Proceedings of the National Academy of Sciences of United States of America 113: 4266-4271. https://doi.org/10.1073/pnas.1602310113

Peralta O, Ortínez-Álvarez A, Basaldud R, Santiago N, Álvarez-Ospina H, de la Cruz K, Barrera V, de la Luz Espinosa M, Saavedra I, Castro T, Martínez-Arroyo A, Páramo, VH, Ruiz-Suárez LG, Vázquez-Gálvez FA, Gavilán A. 2019. Atmospheric black carbon concentrations in Mexico. Atmospheric Research 230: 104626. https://doi.org/10.1016/j.atmosres.2019.104626

Peralta O, Ortínez-Álvarez A, Torres-Jardón R, Suárez-Lastra M, Castro T, Ruiz-Suárez LG. 2021. Ozone over Mexico City during the COVID-19 pandemic. Science of The Total Environment 761: 143183. https://doi.org/10.1016/j.scitotenv.2020.143183

Pöschl U. 2005. Atmospheric eerosols: Composition, transformation, climate and health effects. Angewandte Chemie International Edition 44: 7520-7540. https://doi.org/10.1002/anie.200501122

Prieto C, Álvarez-Ospina H, Salcedo D, Castro T, Peralta O. 2023. Mass absorption efficiency of PM_1 in Mexico City during ACU15. Atmosphere 14: 100. https://doi.org/10.3390/atmos14010100

Ram K, Sarin MM. 2009. Absorption coefficient and site-specific mass absorption efficiency of elemental carbon in aerosols over urban, rural, and high-altitude sites in India. Environmental Science & Technology 43: 8233-8239. https://doi.org/10.1021/es9011542

Ramanathan V, Carmichael G. 2008. Global and regional climate changes due to black carbon. Nature Geoscience 1: 221-227. https://doi.org/10.1038/ngeo156

Salcedo D, Álvarez-Ospina H, Peralta O, Castro T. 2018. PM_1 chemical characterization during the ACU15 campaign, south of Mexico City. Atmosphere 9: 232. https://doi.org/10.3390/atmos9060232

Schumann U. 2012. Atmospheric physics: Background – Methods – Trends (research topics in aerospace). Springer, Berlin. https://doi.org/10.1007/978-3-642-30183-4

Srinivas B, Sarin MM. 2013. Light absorbing organic aerosols (brown carbon) over the tropical Indian Ocean: Impact of biomass burning emissions. Environmental Research Letters 8: 044042. https://doi.org/10.1088/1748-9326/8/4/044042

Tao J, Zhang Z, Wu Y, Lin Z, Cao J, Shen Z, Zhang R. 2018. Characteristics of Mass Absorption Efficiency of Elemental Carbon in Urban Chengdu, Southwest China: Implication for the Coating Effects on Aerosol Absorption. Aerosol Science and Engineering 2: 33-41. https://doi.org/10.1007/s41810-018-0022-8

Tao J, Zhan, Z, Wu Y, Zhang L, Wu Z, Cheng P, Li M, Chen L, Zhang R, Cao J. 2019. Impact of particle number and mass size distributions of major chemical components on particle mass scattering efficiency in urban Guangzhou of South China. Atmospheric Chemistry and Physics 19: 8471-8490. https://doi.org/10.5194/acp-19-8471-2019

Tao J, Surapipith V, Han Z, Prapamontol T, Kawichai S, Zhang L, Zhang Z, Wu Y, Li Jw, Li J, Yang Y, Zhang R. 2020. High mass absorption efficiency of carbonaceous aerosols during the biomass burning season in Chiang Mai of northern Thailand. Atmospheric Environment 240: 117821. https://doi.org/10.1016/j.atmosenv.2020.117821

Torres-Jardón R, García-Reynoso JA, Jazcilevich A, Ruiz-Suárez LG, Keener TC. 2009. Assessment of the ozone-nitrogen oxide-volatile organic compound sensitivity of Mexico City through an indicator-based approach: Measurements and numerical simulations comparison. Journal of the Air & Waste Management Association 59: 1155-1172. https://doi.org/10.3155/1047-3289.59.10.1155

Turpin BJ, Cary RA, Huntzicker JJ. 1990. An in situ, time-resolved analyzer for aerosol organic and elemental carbon. Aerosol Science and Technology 12: 161-171. https://doi.org/10.1080/02786829008959336

Turpin BJ, Huntzicker JJ. 1995. Identification of secondary organic aerosol episodes and quantitation of primary and secondary organic aerosol concentrations during SCAQS. Atmospheric Environment 29: 3527-3544. https://doi.org/10.1016/1352-2310(94)00276-Q

Wang J, Nie W, Cheng Y, Shen Y, Chi X, Wang Jd, Huang X, Xie Y, Sun P, Xu Z, Qi X, Su H, Ding A. 2018. Light absorption of brown carbon in eastern China based on 3-year multi-wavelength aerosol optical property observations and an improved absorption Ångström exponent segregation method. Atmospheric Chemistry and Physics 18: 9061-9074. https://doi.org/10.5194/acp-18-9061-2018

Wang X, Xue Y, Cen B-L, Zhang P, He H-D. 2020. Study on pollutant emissions of mixed traffic flow in cellular automaton. Physica A: Statistical Mechanics and its Applications 537: 122686. https://doi.org/10.1016/j.physa.2019.122686

Weingartner E, Saathoff H, Schnaiter M, Streit N, Bitnar B, Baltensperger U. 2003. Absorption of light by soot particles: Determination of the absorption coefficient by means of aethalometers. Journal of Aerosol Science 34: 1445-1463. https://doi.org/10.1016/S0021-8502(03)00359-8

Zhang, F, Xu L, Chen J, Chen X, Niu Z, Lei T, Li C, Zhao J. 2013. Chemical characteristics of $PM_{2.5}$ during haze episodes in the urban of Fuzhou, China. Particuology 11: 264-272. https://doi.org/10.1016/j.partic.2012.07.001